

Planck Frequency Maps for the Cosmic Microwave Background Observation

Aktaş, Melih
Duque Bran, Andrés Felipe

December 22, 2022

Abstract

The study of the Cosmic Background Radiation (CMB) provides insight into the beginnings of the universe. By processing the data measured by the Planck spacecraft, using the internal linear combination method and the *Healpy* astronomical data management library, it was possible to carry out a study of the CMB. In addition, a qualitative analysis of the domain regime of this type of radiation for a certain frequency range was performed, as well as the estimation of the size of the Point Spread Function (PSF), at the Full Width at Half Maximum (FWHM).

The development of this work can be find at <https://github.com/afduquebr/Planck-2015>.

1 Introduction

1.1 Cosmic Microwave Background

The Cosmic Microwave Background radiation (CMB) is the oldest electromagnetic radiation present in the universe. Its emission origin dates back to the recombination era, which allows us, from its study, to obtain information about the beginning of the universe [1].

1.2 Planck Spacecraft

The Planck satellite is a space telescope that was in operation between 2009 and 2013 to study the CMB at infrared and microwave frequencies [2].

Planck has two instruments to detect the intensity of photons. The Low Frequency Instrument (LFI) covers frequencies of 30, 44 and 70 GHz. And the High Frequency Instrument (HFI) covering frequencies of 100, 143, 217, 353, 545 and 857 GHz to record the CMB.

1.3 Point Spread Function

The Point Spread Function (PSF) describes the response of a system that forms images to an object point source. The PSF diffraction theory is given by the Airy disc, where the intensity is given by the equation

$$I(\theta) = I_0 \left[\frac{J_1(x)}{x} \right]^2,$$

being I_0 the maximum intensity of the Airy disk and J_1 the first order Bessel function [3].

1.4 Healpy

HealPy is a Python library based on *Hierarchical Equal Area isoLatitude Pixelization (HEALPix)*, originally developed as a *C++* package, that allows you to work analytically on data stored in pixelated form on a sphere.

In this work, the use of this tool is of vital importance since it allows to work with maps as one-dimensional arrays and also to be able to apply convolutions, increase or decrease resolutions, visualisation in a Mollweide projection, calculation of the power spectrum of a map, among others [4].

1.5 Gaussian Convolution

The Gaussian Convolution G_σ is a signal process employed for signal and image processing, and is given by

$$(G_\sigma * f)(x) = \int_{-\infty}^{\infty} G_\sigma(x-y) \cdot f(y) dy$$

and

$$G_\sigma(x) = \sqrt{\frac{1}{2\pi\sigma^2}} \cdot e^{-\frac{x^2}{2\sigma^2}},$$

where f is the input signal and σ is the standard deviation of the Gaussian Convolution [5]. In particular, this kind of convolution has a property that allows one convolution to be expressed as the composition of two, which means

$$G_{\sigma_1} * f = G_{\sigma_2} * (G_{\sigma_3} * f),$$

with

$$\sigma_1 = \sqrt{\sigma_2^2 + \sigma_3^2}. \quad (1)$$

1.6 Internal Linear Combination

The Internal Linear Combination method (ILC) is a tool that allows to isolate the amplitude as a function of electromagnetic frequency from multiple frequency observations. It is based on the linear combination of the observations that minimise the variance of the output and at the same time keeps the signal intact [6].

The total emission at a given frequency channel T_i for each pixel p is given by

$$T_i(p) = \sum_{j=1}^{N_s} A_{ij}(p) \cdot S_j(p) + n_j(p),$$

where S_j denotes the maps of the astronomical compounds and n_j denotes the instrumental noise. A_{ij} is the mixing matrix that depends on the j -th compound and the i -th frequency channel.

The ILC allows us to reconstruct the desired signal as a linear combination of the input maps, which means

$$\hat{S}_c(p) = \omega^\top T(p),$$

where ω^\top are the weights of the linear combination. Then, the variance can be calculated as

$$Var(\hat{S}_c) = \omega^\top \langle TT^\top \rangle \omega = \omega^\top C_T \omega,$$

denoting C_T as the covariance matrix of T . And imposing the constrain $\omega^\top f_c = 1$, with f_c depending on the mixing matrix [6]. Then, by means of Lagrange multipliers, one can obtain that

$$\hat{S}_c(p) = \frac{1^\top C_T^{-1}}{1^\top C_T^{-1} 1} \cdot T(p), \quad (2)$$

where 1 is a vector with all of its entries of value 1 .

1.7 Spherical Harmonics

The solution to Laplace's equation

$$\nabla^2 f(\rho, \theta, \phi) = 0,$$

whose solution in spherical coordinates is considered independent for its three variables $f(\rho, \theta, \phi) = R(\rho)Y(\theta, \phi)$ [7]. Thus, the angular solution to this equation is known as the spherical harmonics and are stated by

$$Y_l^m(\theta, \phi) = \sum_{l,m} a_{lm} P_l^m(\cos\theta) e^{im\phi},$$

with P_l^m being the associated Legendre polynomials and

$$a_{lm} = \sqrt{\frac{2l+1}{4\pi} \cdot \frac{(l-m)!}{(l+m)!}}.$$

In the study of the CMB anisotropies [1], the radiation angular power spectrum is defined as

$$C_l = \left\langle |a_{lm}|^2 \right\rangle,$$

however, the value usually plotted for the analysis of this quantity is

$$\frac{l(l+1)}{2\pi} \cdot C_l. \quad (3)$$

2 PSF: Size

The theoretical size of the PSF is calculated by means of the Full Width at Half Maximum (FWHM) approximation, given by the equation

$$\theta_{FWHM} = 1.025 \cdot \frac{\lambda}{d} = 1.025 \cdot \frac{c}{\nu \cdot d}$$

where λ is the wavelength, c is the speed of light, ν is the frequency and $d = 1.5$ m is the diameter of aperture of the PSF. Given this, the angle of aperture for the frequencies of the LFI and HFI are shown in table 2.

ν [GHz]	θ_{FWHM} [arcmin]
30	23.49
44	16.02
70	10.07
100	7.05
143	4.93
217	3.25
353	2.00
545	1.29
857	0.82

Table 1: Theoretical size of the PSF in dependency of the frequencies.

3 Sky Components

The total microwave spectrum in the universe is composed of different sources and components that contribute to the total spectrum in the universe, each can be dominant over the others. For this work, we focus our analysis on the effects of Synchrotron emission, free-free emission, thermal dust emission, the Sunyaev-Zeldovich thermal effect and the CMB. Other sources, such as the kinetic SZ effect do not contribute appreciably to the final total spectrum.

Synchrotron

The Synchrotron is generated by spiralling electrons present in the Galactic Magnetic Field [8]. For frequencies above 20 GHz, it can be easily approximated to a power behaviour close to $\sim \nu^{-3.11}$, as it is possible to appreciate in figure 1. Its expression is given by

$$s_s = A_s \left(\frac{\nu}{\nu_0} \right)^{-3.11}$$

with $A_s = 2.75 K$.

Free-free

The Free-free emission, also known as Bremsstrahlung is generated by electron-ion collisions that emit a photon causing the electron to decelerate. When the frequency values are low, a constant behaviour is expected. Nevertheless, for high order frequencies, it is approximately $\sim \nu^{-2.15}$ [8]. Its expression is given by

$$g_{ff} = \log\{\exp[5.960 - \sqrt{3}/\pi \log(\nu_9 T_4^{-3/2})] + e\},$$

$$\tau = 0.05468 T_e^{-3/2} \nu_9^{-2} EM g_{ff},$$

$$s_{ff} = 10^6 T_e(1 - e^{-\tau}).$$

The behaviour of this kind of radiation can be appreciated in figure 2.

Thermal Dust

The Thermal Dust is calculated from the temperature of dust grains, it highly depends in parameters such as dust population and environment. It is fitted as a modified black body, however, above frequencies of 857 GHz, this behaviour is no longer accurate since the modelling of dust particles results into something more difficult. Its expression is given by

$$\gamma = \frac{h}{k_B T_d},$$

$$s_d = A_d \cdot \left(\frac{\nu}{\nu_0}\right)^{\beta_d-1} \frac{\exp(\gamma\nu_0) - 1}{\exp(\gamma\nu) - 1}.$$

The behaviour of this kind of radiation can be appreciated in figure 3.

Thermal SZ

The Sunyaev-Zeldovich effect is caused by photons that escape from hot electrons, and which no longer correspond to a black body radiation. In this special case, the spectrum relies on the scattering parameter for these photons. For frequencies above 217 GHz it is positive. Its expression is given by

$$s_{sz} = 10^6 y_{sz}/g(\nu) T_{CMB} \left(\frac{x(\exp(x) + 1)}{\exp(x) - 1} - 4 \right).$$

The behaviour of this kind of radiation can be appreciated in figure 4.

CMB

The CMB is described by black-body radiation with the only parameter being the temperature $T = 2.7255 \pm 0.0006 K$ [8]. Due to its high accuracy, other effects are neglected. Its expression is given by

$$x = \frac{h\nu}{k_B T_{CMB}},$$

$$g(\nu) = (\exp(x) - 1)^2 / (x^2 \exp(x)),$$

$$s_{CMB} = A_{CMB}/g(\nu).$$

The dominance over the other emissions is highly appreciated in figure 5. In any other case it can be comparable, since it appears with dashed line in any other plot.

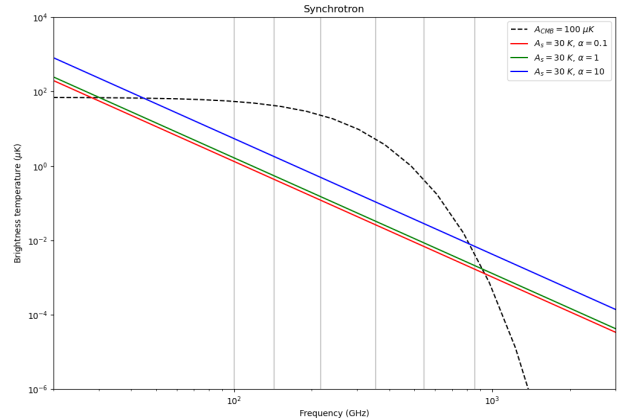


Figure 1: Spectral energy densities for synchrotron emission in brightness temperature, for several combination of parameters. Vertical grey lines indicate the high frequency instrument frequencies.

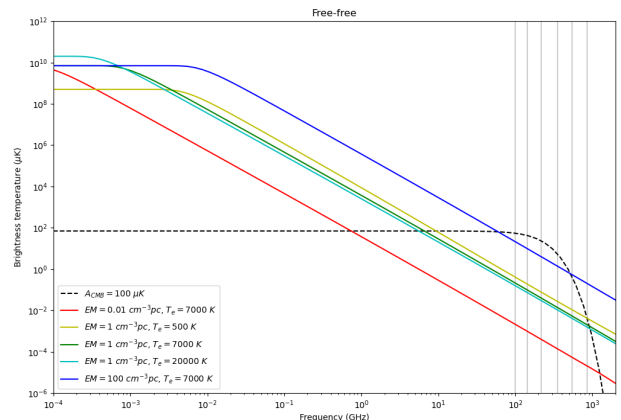


Figure 2: Spectral energy densities for free-free emission in brightness temperature, for several combination of parameters. Vertical grey lines indicate the high frequency instrument frequencies.

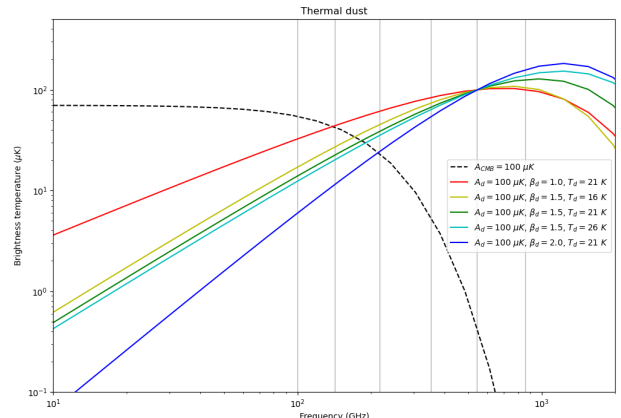


Figure 3: Spectral energy densities for thermal dust emission in brightness temperature, for several combination of parameters. Vertical grey lines indicate the high frequency instrument frequencies.

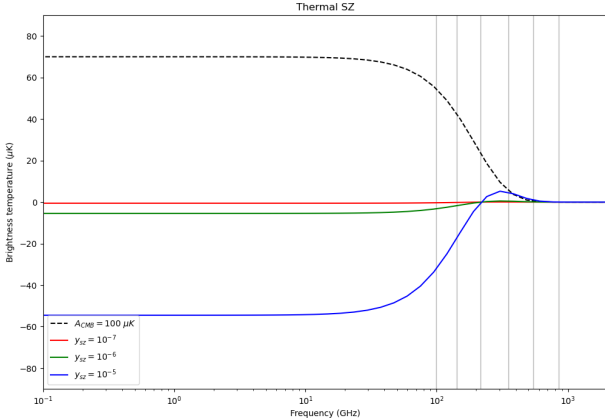


Figure 4: Spectral energy densities for the thermal Sunyaev-Zeldovich effect in brightness temperature, for several combination of parameters. Vertical grey lines indicate the high frequency instrument frequencies.

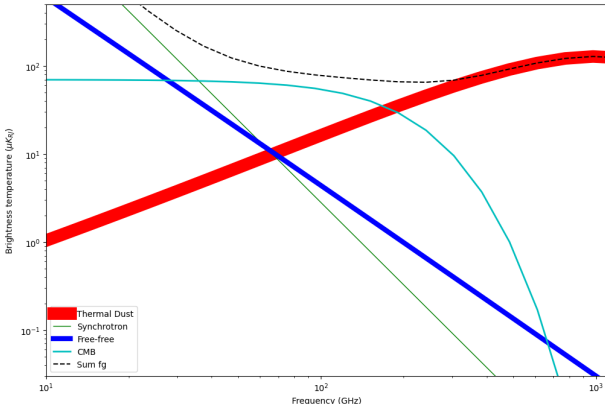


Figure 5: Brightness temperature rms as a function of frequency. The values for each contribution were found by simply getting the average value from the corresponding given set of parameters.

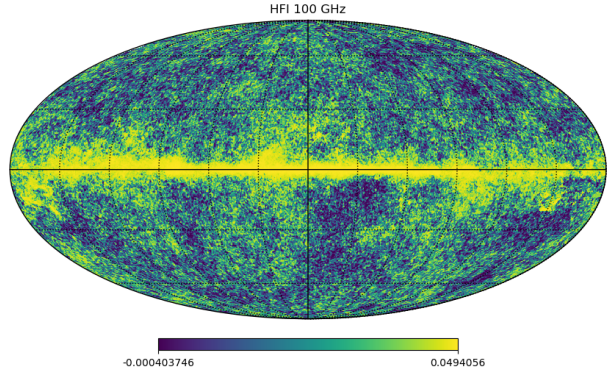


Figure 6: Mollweide view of the 100 GHz frequency map.

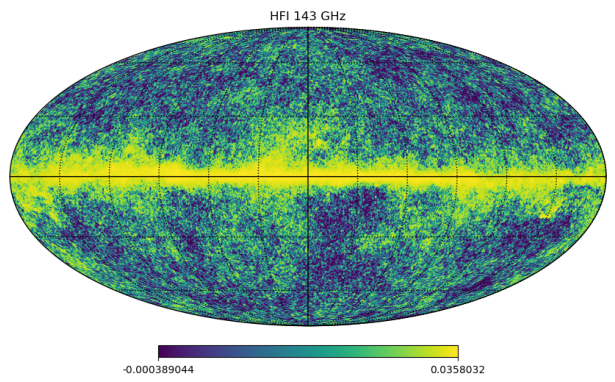


Figure 7: Mollweide view of the 143 GHz frequency map.

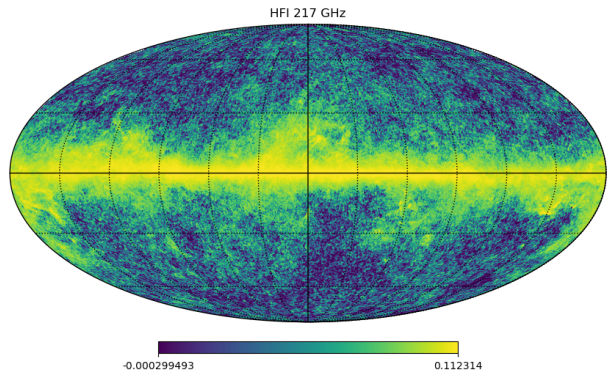


Figure 8: Mollweide view of the 217 GHz frequency map.

4 The Planck Maps

Hereinafter, we will mostly be relying on the *Healpy* library (1.4). As we want to employ the ILC (1.6) method in order to extract the CMB map, we first start of by convolving the FWHM values of the individual maps for every frequencies taken by the high frequency instrument to the same value which is 10 arc minutes. We make the convolutions by virtue of equation (1). Note that for the preexisting FWHM values, we do not use the theoretical values computed at (2) but use the ones given in the dataset. Also, as it will be easier to work with, we degrade the *nside* values of the maps to 512 from 2048. We make the mapping in Mollweide projection with "ring" ordering scheme. Here are the results,

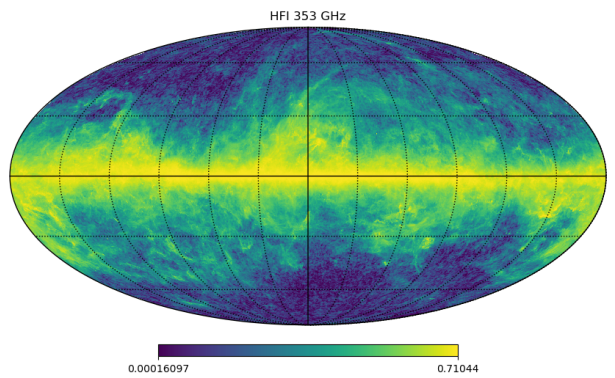


Figure 9: Mollweide view of the 353 GHz frequency map.

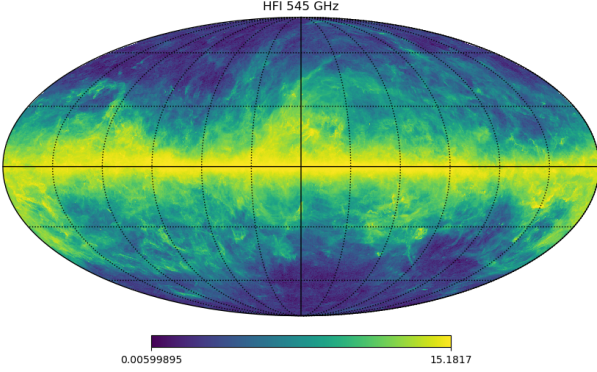


Figure 10: Mollweide view of the 545 GHz frequency map.

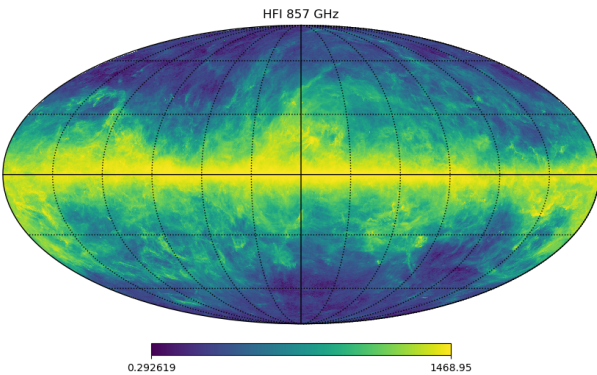


Figure 11: Mollweide view of the 857 GHz frequency map.

For the cases of 545 GHz and 857 GHz, in order to align their units with the others, namely, K_{CMB} , we divided them by 58.04 and 2.27 respectively.

5 The CMB Maps

Now that we have the total emission absorbed for all frequencies, we can finally extract the CMB contribution from them using the ILC method, in particular equation (2). Here is the resulting CMB map,

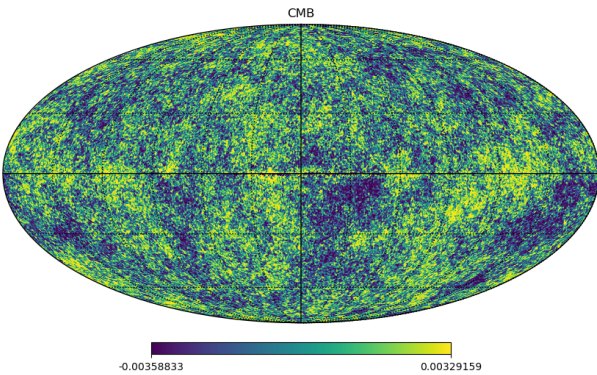


Figure 12: Mollweide view of the CMB map.

Moreover, to get an even clearer description of the CMB contribution, we can filter out the galaxies from the map. As the galaxies are the most dominant in the 857 GHz range, we will use this map to filter them out. In order to do so, we will set the points with temperature greater than the average value of the map, equal to 0 and the rest

equal to 1. This is due to the fact that the galaxies are the brightest region in the sky. Then, we will multiply the original CMB map with this masking map to achieve the desired picture. This technique is referred to as "masking". Namely,

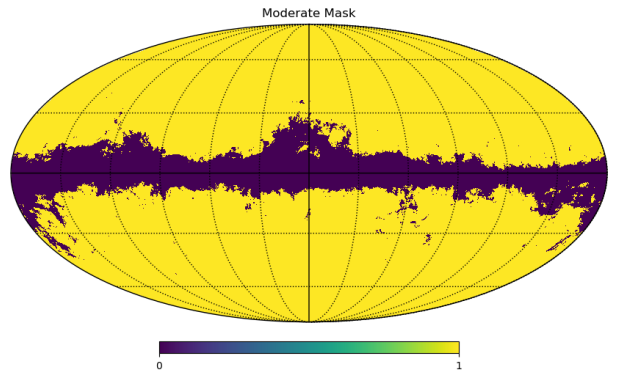


Figure 13: Mollweide view of the masking map.

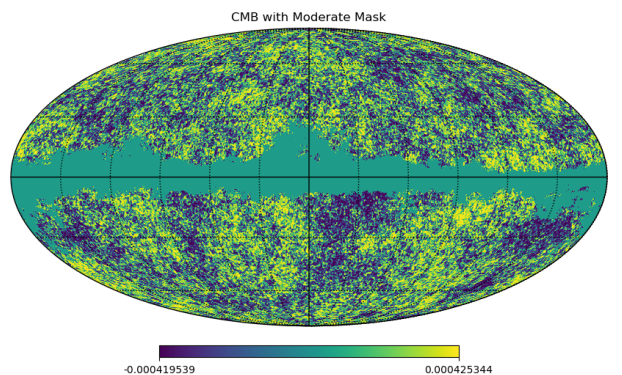


Figure 14: Mollweide view of the moderate masked CMB map.

In order to investigate the effects of masking further, we will also employ a slightly greater and smaller masks. To do so, we simply multiply the threshold between the zeros and ones with, say, 0.4 and 2.1 for the big and the small mask respectively. Here are the resulting masked CMB maps,

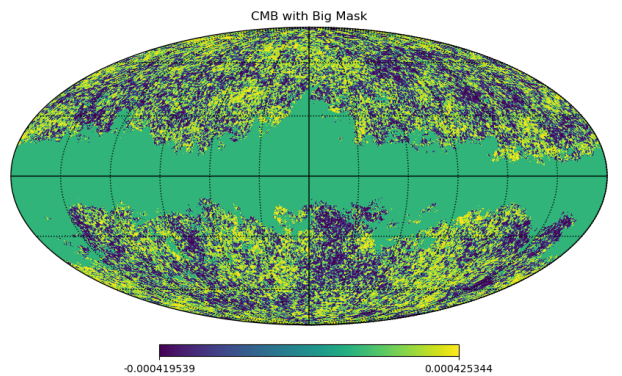


Figure 15: Mollweide view of the big masked CMB map.

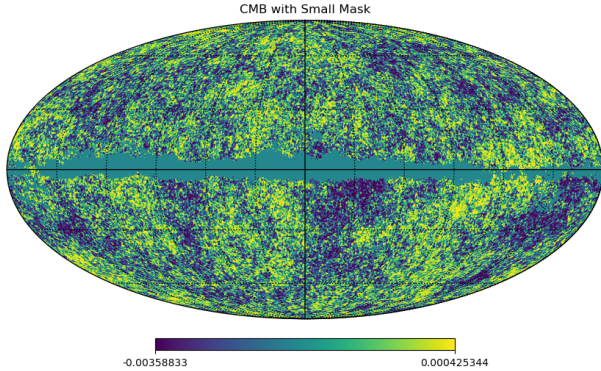


Figure 16: Mollweide view of the small masked CMB map.

6 Harmonic Spheres

There are quite convenient *Healpy* functions which will allow us to employ the results of the aforementioned section of spherical harmonics on our maps and find their power spectra, see equation (3). Before transforming the previously measured CMB maps to their spherical harmonics, we revert their *nside* value back to 2048 to get a clearer graph. Here are the results, However, these are merely

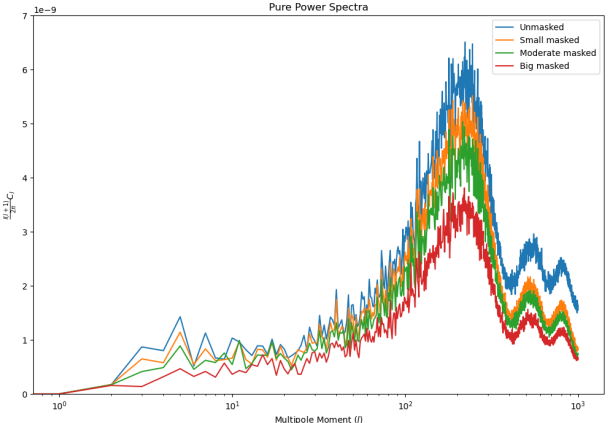


Figure 18: Power spectra of the pure CMB maps with log scaled x axis.

The effect of the masking can easily be observed on the power spectra. Going from unmasked to big masked, in figure (6), one can see a trend of decrease, as expected. In fact, as a further direction to this report, one can introduce a numerical function for the effect of the masking by employing various sizes of masks, a lot more than 3, and measuring their effects on the power spectrum.

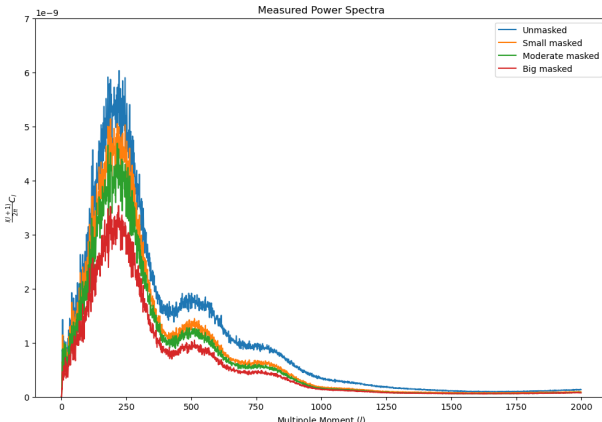


Figure 17: Power spectra of the measured CMB maps.

the power spectra of the measured sky and not the ones we are interested in. We want to get the pure sky power spectra. In order to do so, we must revert every modification caused by our measurement device. Namely, the pixelization of *nside* = 2048 and the convolution of 10 arc minutes. Again, there are quite convenient functions in the *Healpy* library (*pixwin*, *gauss_beam*) which will help us revert back to the pure forms of the power spectra. Here are the final results,

7 Conclusion

In this analysis, by using various functions from the *Healpy* library, which proved to be quite rich and user friendly, we employed the ILC method on the data collected by the Planck satellite and were able to find an elegant result for the CMB map, albeit ignoring any noise contributions. Moreover, the masking we did using the 857 GHz map was quite efficient since the contribution to CMB at that frequency is negligible, as can be justified from figure (5).

References

- [1] Andrew Liddle. *An introduction to modern cosmology*; 2nd ed. Chichester: Wiley, 2003.
- [2] *Planck*. https://www.esa.int/Enabling_Support/Operations/Planck. Accessed: 2022-12-19.
- [3] *Airy Disk*. <https://en.wikipedia.org/wiki/Airy-disk>. Accessed: 2022-12-19.
- [4] *Healpy Documentation*. <https://healpy.readthedocs.io/en/latest/index.html>. Accessed: 2022-12-16.
- [5] Pascal Getreuer. “A Survey of Gaussian Convolution Algorithms”. In: *Image Processing On Line* 3 (2013). <https://doi.org/10.5201/ipol.2013.87>, pp. 286–310.
- [6] G. Hurier, J. F. Macías-Pérez, and S. Hildebrandt. “MILCA, a modified internal linear combination algorithm to extract astrophysical emissions from multifrequency sky maps”. In: *Astronomy & Astrophysics* 558 (2013), A118. DOI: 10.1051/0004-6361/201321891. URL: <https://doi.org/10.1051/0004-6361/201321891>.
- [7] *The Spherical Harmonics*. http://scipp.ucsc.edu/~haber/ph116C/SphericalHarmonics_12.pdf. Accessed: 2022-12-20.
- [8] Planck Collaboration. “Planck 2015 results”. In: *Astronomy & Astrophysics* 594 (2016), A10. DOI: 10.1051/0004-6361/201525967. URL: <https://doi.org/10.1051/0004-6361/201525967>.